Reduction of the Hodgkin-Huxley Equations to a Single-Variable Threshold Model

Werner Kistler, Wulfram Gerstner, and J. Leo van Hemmen
Institut für Theoretische Physik
Physik-Department der TU München
D-85748 Garching bei München
Germany

August 9, 1996

Abstract

It is generally believed that a neuron is a threshold element which fires when some variable u reaches a threshold. Here we pursue the question of whether this picture can be justified and study the four-dimensional neuron model of Hodgkin and Huxley as a concrete example. The model is approximated by a response kernel expansion in terms of a single variable, the membrane voltage. The first-order term is linear in the input and has the typical form of an elementary postsynaptic potential. Higher-order kernels take care of nonlinear interactions between input spikes. In contrast to the standard Volterra expansion the kernels depend on the firing time of the most recent output spike. In particular, a zero-order kernel which describes the shape of the spike and the typical afterpotential is included. Our model neuron fires, if the membrane voltage, given by the truncated response kernel expansion crosses a threshold. The threshold model is tested on a spike train generated by the Hodgkin-Huxley model with a stochastic input current. We find that the threshold model predicts nearly 90 percent of the spikes correctly. Our results show that, to good approximation, the description of a neuron as a threshold element can indeed be justified.

Keywords:
Hodgkin-Huxley equations, Volterra series, spiking neurons, threshold

1 Introduction

Neuronal activity is the result of a highly nonlinear dynamic process that was first described mathematically by Hodgkin and Huxley (1952), who proposed a set of four coupled differential equations. The mathematical analysis of these and other coupled nonlinear equations is known to be a hard problem and an intuitive understanding of the dynamics is difficult to obtain. Hence, a simplified description of neuronal activity is highly desirable and has been attempted repeatedly, e.g., by FitzHugh (1961), Rinzel (1985), Abbott and Kepler (1990), Av-Ron et al. (1991), Kepler et al. (1992), Joeken and Schwegler (1995) – to mention only a few. An example of a simple model of neuronal spike dynamics is the integrate-and-fire neuron, which dates back to Lapicque as early as 1907 and has become quite popular in neural networks modeling; see e.g., Usher et al. (1993), Abbott and van Vreeswijk (1993), Tsodyks et al. (1993), Hopfield and Herz (1995).

In this paper we aim at a generalized, and realistic, version of the integrate-and-fire model. In order to reduce the four nonlinear equations of Hodgkin and Huxley to a simplified model with a single, scalar variable u, we use the *spike response method*, which has been introduced previously (Gerstner 1991, Gerstner and van Hemmen 1992, Gerstner 1995). A spike is triggered at a time t^f, if the membrane potential u approaches a threshold ϑ from below. For $t > t^f$ and t^f being the *most recent* firing time, the membrane voltage u in the reduced description is given by an expansion of the form,

$$u(t) = \eta(t - t^f) + \int_0^\infty \mathrm{d}s\ \epsilon^{(1)}(t - t^f; s)\, I(t - s) + \dots \tag{1}$$

The following spike is generated if $u(t) = \vartheta$ and $\frac{d}{dt}u(t) > 0$, which defines the next firing time t^f, and so on. The kernels η and ϵ have a direct neuronal interpretation. The first term $\eta(t-t^f)$ in the right-hand side of (1) describes the form of a spike and the typical afterpotential following it. The action potential is triggered at $t = t^f$, it reaches its maximum after a time δ and it is followed by a period of hyperpolarization that extends over approximately 15 ms; cf. Fig. 1a. From a different point of view, we can think of $\eta(t - t^f)$ as the neuron's response to the threshold crossing at t^f. Similarly, the kernel ϵ describes the response of the membrane potential to an input current I. More precisely, $\epsilon_1^{(1)}(\infty; s)$ as a function of s is the linear response to a *small* current pulse at time $s = 0$ given that the neuron did not fire in the past. In biological terms, $\epsilon^{(1)}$ describes the form of the postsynaptic potential evoked by an input spike; cf. Fig. 1b. Since the responsiveness of the membrane to input pulses is reduced during or shortly after an action potential, the form of the postsynaptic potential depends also on the time $t - t^f$ that has passed since the last output spike. Higher-order terms in Eq. (1) describe the nonlinear interaction between several input pulses.

$1a$

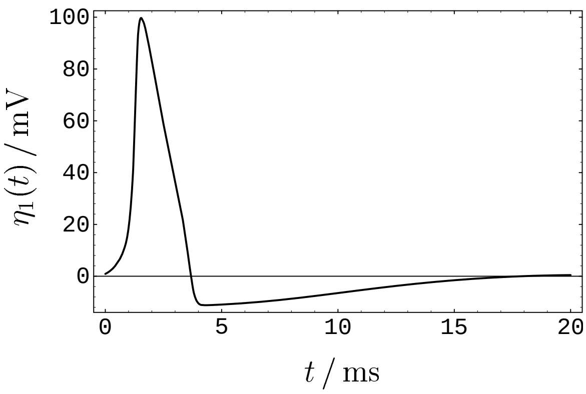

$1b$

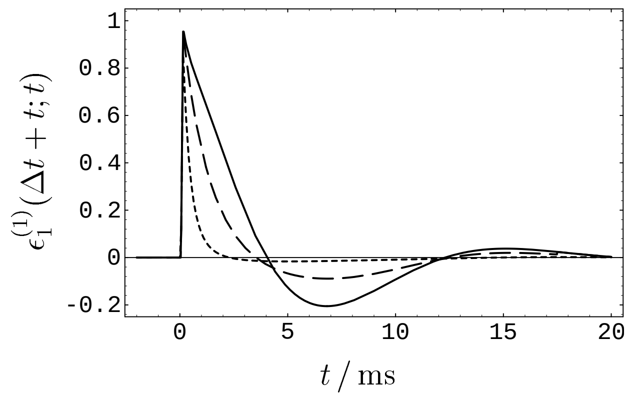

Figure 1: Kernels corresponding to the Hodgkin-Huxley equations and obtained by the methods described in this paper.
a. The kernel η_1 describes the typical shape of a spike and the afterpotential. The spike has been triggered at time $t = 0$.
b. The first-order kernel $\epsilon_1^{(1)}$ describes the form of the postsynaptic potential. The solid line in Fig. 1b shows the postsynaptic potential evoked by a short pulse of unit strength that has arrived at time $t = 0$ while *no* spikes had been generated in the past. If there was an output spike $\Delta t = 6.5\,\mathrm{ms}$ (dotted line) or $\Delta t = 10.5\,\mathrm{ms}$ (dashed line) before the arrival of the input pulse, the response is significantly reduced. The solid line corresponds to $\Delta t = \infty$.

In the following, we concentrate on the four-dimensional set of equations proposed by Hodgkin and Huxley to describe the spike activity in the giant axon of the squid (Hodgkin and Huxley 1952). We consider it as a well-studied standard model of spike activity, even though it does not provide a correct description of spiking in cortical neurons of mammals. The methods introduced below are, however, more general and can also be applied to more detailed neuron models which often involve tens or hundreds of variables (Yamada et al. 1989, Wilson et al. 1989, Traub et al. 1991, Ekeberg et al. 1991).

2 Theoretical framework

2.1 Standard Volterra Expansion

In order to approximate the membrane voltage u of the Hodgkin-Huxley equations, we start with a Volterra expansion (Volterra 1959),

$$u(t) = \int_0^\infty \mathrm{d}s\ \epsilon_0^{(1)}(s) I(t-s) + \frac{1}{2!} \int_0^\infty \mathrm{d}s \int_0^\infty \mathrm{d}s'\ \epsilon_0^{(2)}(s,s') I(t-s) I(t-s') + \ldots \quad (2)$$

The first-order term $\epsilon_0^{(1)}(s)$ describes the membrane's linear response to an external input current $I(t)$, the second-order term $\epsilon_0^{(2)}(s,s')$ takes into account nonlinear interactions between inputs at two different times, and the following terms take care of higher-order nonlinearities. We would like to stress that (2) is an ansatz whose usefulness we still have to verify. It is by no means evident that the series converges reasonably fast.

2.2 Expansion during and after spikes

When dealing with series expansions, we have to examine their convergence. As we will see later on, the expansion (2) converges as long as the input is so weak that *no* spikes are generated. If a spike is triggered at time t^f by some strong input, the neuronal dynamics jumps onto a trajectory in phase space that is always (nearly) the same, viz., the action potential. During the spike the evolution is determined by nonlinear intrinsic processes and is hardly influenced by external input. We, therefore, replace (2) by

$$u(t) = \eta_1(t-t^f) + \int_0^\infty \mathrm{d}s\; \epsilon_1^{(1)}(t-t^f;s) I(t-s) + \\ + \frac{1}{2!}\int_0^\infty \mathrm{d}s \int_0^\infty \mathrm{d}s'\; \epsilon_1^{(2)}(t-t^f;s,s') I(t-s) I(t-s') + \dots \quad (3)$$

Here $\eta_1(t-t^f)$ describes the evolution of the membrane potential during the spike and the relaxation process thereafter. In biological terms, $\eta_1(t-t^f)$ gives the form of a spike and the afterpotential. As in (2), the term $\epsilon_1^{(1)}$ describes the membrane's linear response to an input $I(t)$. Since inputs are much less effective during and shortly after a spike, the term $\epsilon_1^{(1)}$ depends upon the time $t-t^f$ which has passed since the spike was triggered at t^f. The ϵ's are called *response kernels*. The formal arguments justifying (3) are discussed in the Appendix.

The lower index of $\epsilon_1^{(1)}$ indicates that we take into account the effects of the most recent spike only. We can systematically increase the accuracy of our description, if we include more and more spikes that have occured in the recent past. Taking into account the most recent p spikes we would have

$$u(t) = \eta_p(t-t_1^f, \dots, t-t_p^f) + \\ + \int_0^\infty \mathrm{d}s\; \epsilon_p^{(1)}(t-t_1^f,\dots,t-t_p^f;s) I(t-s) + \\ + \frac{1}{2!}\int_0^\infty \mathrm{d}s \int_0^\infty \mathrm{d}s'\; \epsilon_p^{(2)}(t-t_1^f,\dots,t-t_p^f;s,s') I(t-s) I(t-s') + \dots \quad (4)$$

In general, $\eta_p(\sigma_1,\dots,\sigma_p)$ is a complicated function of the p arguments. Since we expect that adaptation is the dominant effect we make the ansatz

$$\eta_p(\sigma_1,\dots,\sigma_p) = \sum_{k=1}^{p} \eta_1(\sigma_k) \; . \quad (5)$$

Here $\eta_1(\sigma)$ describes a single spike and its afterpotential. A linear summation of the afterpotentials of several preceding spikes is often sufficient to describe the well-known adaptation effects of neuronal activity (Gerstner and van Hemmen 1992, Ekeberg et al. 1991, Kernell and Sjöholm 1973).

Below we will show that for the Hodgkin-Huxley model excellent results are achieved with Eq. (3), that is, with $p = 1$. In other words, only the most recent output spike affects the dynamics. This is not too surprising since the Hodgkin-Huxley equations show no pronounced adaptation effects.

2.3 Relation to integrate-and-fire models

In passing we note that the integrate-and-fire model is a special case of Eq. (3) with the response kernels (Gerstner 1995)

$$\begin{aligned}\eta_1(\sigma) &= u_0 \exp(-\sigma/\tau)\,\Theta(\sigma), \\ \epsilon_1^{(1)}(\sigma;s) &= \tau^{-1} \exp(-s/\tau)\,\Theta(s)\,\Theta(\sigma-s),\end{aligned} \tag{6}$$

where u_0 is the voltage to which the system is reset after a spike, τ is the membrane time constant, and $\Theta(.)$ is the Heaviside step function with $\Theta(s) = 1$ for $s > 0$ and 0 otherwise. Since except at firing the standard integrate-and-fire model is linear, the determination of the kernels is simple. In particular, all terms beyond $\epsilon_1^{(1)}$ vanish.

Equation (6) applies to the 'one-step' integrate-and-fire model without synaptic or dendritic integration, but generalizations are straightforward. We mention three types of generalization.

(i) The synaptic input current is not a δ-pulse but described by a broad pulse $\alpha(s)$ where $s = 0$ is the time of presynaptic spike arrival. In this case the response kernel $\epsilon_1^{(1)}$ has a finite rise time which is proportional to the width of the input pulse α.

(ii) Similarly, dendritic integration can be incorporated by a broad input pulse $\tilde{\alpha}$. The effect is the same as in (i).

(iii) Finally, we can include a time-dependent threshold $\vartheta_0 + \vartheta(\sigma)$ where σ is the time that has passed since the last output spike.

Points (i) and (ii) are not relevant for a comparison with the Hodgkin-Huxley model, since the equations of Hodgkin and Huxley do not describe synaptic or dendritic transmission processes either. With respect to point (iii), it is easy to see that a time-dependent threshold is equivalent to changing the form of the η_1-kernel. The firing condition is

$$\int_0^\infty \mathrm{d}s\; \epsilon_1^{(1)}(\sigma;s) I(t-s) + \eta_1(\sigma) = \vartheta_0 + \vartheta(\sigma). \tag{7}$$

Subtracting $\vartheta(\sigma)$ on both sides of the equation leads back to (1) with $\eta(\sigma) = \eta_1(\sigma) - \vartheta(\sigma)$.

In section 4.3, we test the performance of integrate-and-fire models with and without time-dependent threshold on a scenario with a fluctuating input current and compare the results with the Hodgkin-Huxley model.

2.4 Derivation of the kernels

For complicated neuron models described by several nonlinear differential equations, the kernels can be derived systematically by the following procedure. In order to compute the response kernel $\epsilon_0^{(1)}$, we linearize the equations around the constant solution $u(t) = \overline{u}$ with zero input $I(t) = 0$. The kernel $\epsilon_0^{(1)}$ is the voltage component of the Green's function of the linearized equation. Second and higher-order kernels can be obtained analytically by more involved methods. The mathematical details can be found in the Appendix.

We have explicitly calculated the kernels $\epsilon_0^{(1)}, \dots, \epsilon_0^{(3)}$ for the Hodgkin-Huxley equations using a computer algebra system. Albeit the length of the expressions grows rather fast – the third-order kernel has about 400 simple terms – we found it more convenient, faster, and less computer memory consuming to calculate the kernels analytically than using a numerical procedure.

It is instructive, however, to see how the kernels can be obtained numerically. To get the linear kernel, we solve the Hodgkin-Huxley equations numerically for an input current $I(t) = c\ i_{t_0}(t)$, where $i_{t_0}(t)$ is a short current pulse of unit strength at t_0, e.g., $i_{t_0}(t) = \tau^{-1}\ \Theta(t - t_0 + \tau/2)\ \Theta(\tau/2 - t + t_0)$ with $\tau \ll 1$ ms. This is an approximate δ-function. We denote the voltage component of the solution by $u[c\, i_{t_0}](t)$ and set $\epsilon_0^{(1)}(t) = \{u[c\, i_{t_0}](t - t_0) - \overline{u}\}\, /\, c$ in the limit $c \to 0$ and $\tau \to 0$, where $\overline{u}$ is the steady-state solution for zero input current. In a similar vein, we measure the voltage response to two current pulses so as to find $\epsilon_0^{(2)}$.

The *improved* kernel $\epsilon_1^{(1)}$ can only be found numerically. This is done in a similar way as above. We use an input current made up of two current pulses, i.e., $I(t) = c_1\, i_{t_1}(t) + c_2\, i_{t_2}(t)$. The first pulse at t_1 is strong enough to generate an output spike at t^f. The membrane potential after the spike serves as a reference trajectory $u[c_1\, i_{t_1}]$. Now we add the second pulse at time t_2 and consider the difference

$$\delta u = \lim_{\substack{c_2 \to 0 \\ \tau \to 0}} c_2^{-1}\ \{u[c_1\, i_{t_1} + c_2\, i_{t_2}] - u[c_1\, i_{t_1}]\}\,. \tag{8}$$

The difference $\delta u(t)$ gives the values of the linear response kernel $\epsilon_1^{(1)}(\sigma; s)$ on a 'diagonal line' with $(\sigma; s) = (s + t_2 - t^f; s)$, namely

$$\epsilon_1^{(1)}(s + t_2 - t^f; s) = \delta u(s + t_2). \tag{9}$$

The procedure is repeated for variable offsets $t_2 - t^f$ by changing the interval between the first and the second pulse. Since the effect of the spike at t^f decreases for $t \gg t^f$, we have

$$\lim_{\sigma \to \infty} \epsilon_1^{(1)}(\sigma; s) = \epsilon_0^{(1)}(s) \tag{10}$$

where $\epsilon_0^{(1)}(s)$ is the analytically derived kernel introduced above.

Finally, the kernel η is determined by solving the Hodgkin-Huxley equations numerically with input $I(t) = c\ i_{t_0}(t)$. The amplitude c has been chosen sufficiently large so as to evoke a spike. The exact value of c is not important. We set $\eta_1(t - t^f) = \lim_{\tau\to 0} u[c\ i_{t_0}](t) - \overline{u}$ for $t > t_0$ where t^f is the time when $u[c\ i_{t_0}](t)$ crosses a formal threshold ϑ and $\bar{u}$ is the constant solution with zero input. Once the amplitude c is fixed, the kernel η is uniquely determined as the form of an action potential with, apart from the triggering pulse, zero input current.

The only free parameter is the threshold ϑ which is to be found by an optimization procedure described below.

2.5 Comparison with Wiener expansions

The approach indicated so far shows that all kernels can be found by a systematic and straightforward procedure. The kernels can be derived either analytically as described in the Appendix or numerically by studying the system's response to input pulses on a *small* set of examples.

This is in contrast to the Wiener theory (Wiener 1958, Palm and Poggio 1977), which analyses the response of a system to Gaussian white noise. Since Wiener's approach to the description of nonlinear systems is a stochastic one, the determination of the Wiener kernels requires large sets of input and output data (Palm and Poggio 1978, Korenberg 1989). Exploiting the deterministic response of the system to well-designed inputs (viz., short pulses) thus simplifies things significantly. The study of impulse response functions is, of course, a well-known approach to linear or weakly nonlinear systems. Here we have extended this approach to highly nonlinear systems under the proviso that the response kernels ϵ are (almost everywhere) continuous functions of their arguments.

It is important to keep in mind that both Volterra and Wiener series cannot fully reproduce the threshold behavior of spike generation, even if higher-order terms are taken into account. The reason is that these expansions can only approximate mappings that are 'smooth', whereas the mapping from input current $I(t)$ to the time course of the membrane voltage has an apparent discontinuity at the spiking threshold; cf. Fig. 2. Of course, this is not a discontinuity in the mathematical sense, but the output is very sensitive to small changes in the input current. We have to correct for this by adding the kernel η each time the series expansion indicates that a spike will occur, say, by crossing an appropriate threshold value. In doing so, we no longer expand around the constant solution $u(t) \equiv 0$, but around $u(t) = \eta(t - t^f)$, i.e., the time course of a standard action potential.

The general framework outlined in this section will now be applied to the Hodgkin-Huxley equations.

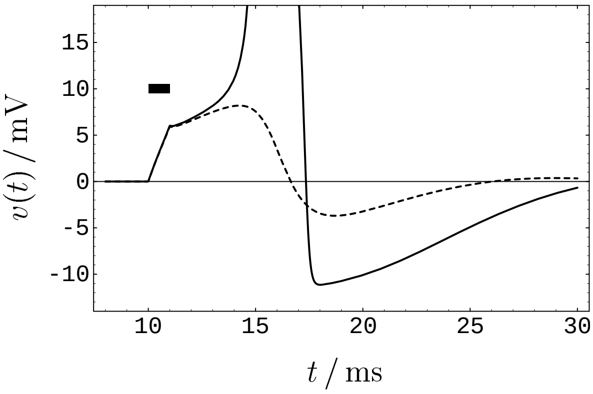

Figure 2: Threshold behavior of the Hodgkin-Huxley equations (11) and (12). We show the response of the Hodgkin-Huxley equations to a current pulse of 1 ms duration. A current amplitude of $7.0\,\mu$A cm^{-2} suffices to evoke an action potential (solid line; the maximum at 100 mV is out of scale), whereas a slightly smaller pulse of $6.9\,\mu$A cm^{-2} fails to produce a spike (dashed line). The time course of the membrane voltage is completely different in both cases. Therefore, the mapping of the input current onto the time course of the membrane voltage is highly sensitive to changes in the input around the spiking threshold. The bar in the upper left indicates the duration of the input pulse.

3 Application to Hodgkin-Huxley equations

In the following we apply the theoretical analysis to the Hodgkin-Huxley equations. First we specify the equations and then we explain how the reduction to the spike response model is performed.

3.1 Hodgkin-Huxley spike trains

According to Hodgkin and Huxley (Hodgkin and Huxley 1952, Cronin 1987), the voltage $v(t)$ across a small patch of axonal membrane, e.g., close to the hillock, changes at a rate given by

$$C\,\frac{dv}{dt} = I(t) - g_{Na}\,m^3\,h\,(v - v_{Na}) - g_K\,n^4\,(v - v_K) - g_L\,(v - v_L), \tag{11}$$

where $I(t)$ is a time-dependent input current. The constants v_{Na}, v_K, and v_L are the equilibrium potentials of the three components sodium, potassium, and 'leakage', and the g's are parameters of the respective ion conductances. The variables m, n, and h change according to a differential equation of the form

$$\frac{dx}{dt} = \alpha_x(v)\,(1 - x) - \beta_x(v)\,x \tag{12}$$

x	v_x	g_x
Na	115mV	120mS/cm^2
K	-12mV	36mS/cm^2
L	10.6mV	0.3mS/cm^2

x	$\alpha_x(v\,/\,\text{mV})$	$\beta_x(v\,/\,\text{mV})$
n	$(0.1 - 0.01\,v)\,/\,[\exp(1 - 0.1\,v) - 1]$	$0.125\exp(-v\,/\,80)$
m	$(2.5 - 0.1\,v)\,/\,[\exp(2.5 - 0.1\,v) - 1]$	$4\exp(-v\,/\,18)$
h	$0.07\exp(-v\,/\,20)$	$1\,/\,[\exp(3 - 0.1\,v) + 1]$

Table 1: The parameters of the Hodgkin-Huxley equations. The membrane capacity is $C = 1\mu\text{F/cm}^2$.

with $x \in \{m, n, h\}$. The parameters are given in Table 1.

For a biological neuron that is part of a larger network of neurons, the input current is due to spike input from many presynaptic neurons. Hence the input current is not constant but fluctuates. In our simulations, we therefore use an input current generated by the following procedure. Every 2 ms, a random number is drawn from a Gaussian distribution with zero mean and standard deviation σ. The discrete current values at intervals of 2 ms are linearly interpolated and define the input $I(t)$. This approach is intended to mimic the effect of spike input into the neuron. The procedure is somewhat arbitrary but easily implementable and leads to a spike train with a broad interval distribution and realistic firing rates depending on σ, as is shown in Fig. 3.

We emphasize that our single-variable model is intended to reproduce the *firing times* of the spikes generated by the Hodgkin-Huxley equations. This is a harder problem than fitting the gain function for *constant* input current.

3.2 Approximation by a threshold model

We want to reduce the four Hodgkin-Huxley equations (11) and (12) to the spike response model (3) in such a way that the model generates a spike train identical with or at least similar to the original one of Fig. 3a. The reduction will involve four major steps. First, we calculate the response functions $\epsilon_0^{(1)}$, $\epsilon_0^{(2)}$, and $\epsilon_0^{(3)}$. We then derive the kernel η_1 and analyze the corrections to $\epsilon_0^{(1)}$ that are caused by the most recent output spike. Finally, we determine a threshold criterion for firing. Before starting, we note that for $I(t) \equiv 0$, the Hodgkin-Huxley equations allow a stationary solution with constant values $v(t) = \overline{v}$, $m(t) = \overline{m}$, $h(t) = \overline{h}$, 3a

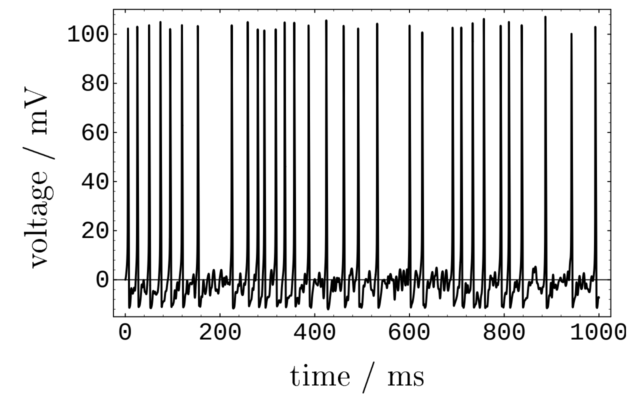

3b

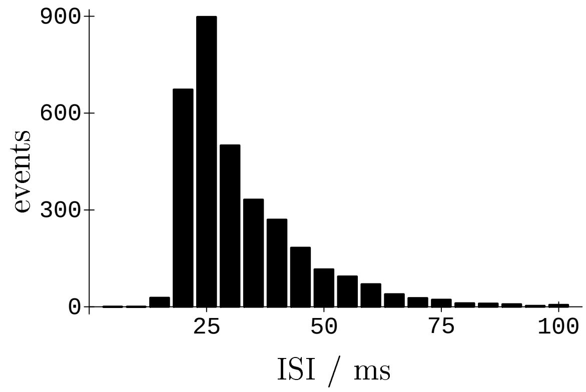

Figure 3: Hodgkin-Huxley model. Figure 3a shows 1000 ms of a simulation of the Hodgkin-Huxley equations stimulated through a fluctuating input current $I(t)$ with zero mean and standard deviation $3\mu\mathrm{A/cm}^2$. Because of the fluctuating input, the spikes occur at stochastic intervals with a broad distribution. A histogram of the inter-spike interval (ISI) sampled over a period of 100 s is plotted in Fig. 3b.

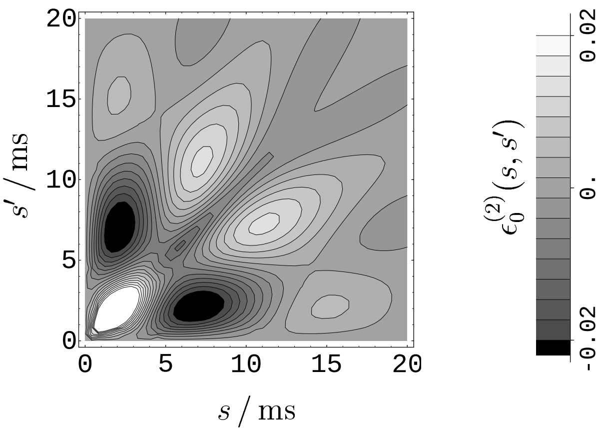

Figure 4: Second-order kernel for the Hodgkin-Huxley equations. The figure exhibits a contour plot for the second-order kernel $\epsilon_0^{(2)}(s, s')$. The kernel vanishes identically for negative arguments, as is required by causality.

and $n(t) = \overline{n}$. The constant solution is stable if $I(t)$ is smaller than a threshold value $I_\vartheta = 9.47\,\mu\text{A/cm}^2$, which is determined by the parameter values given in Table 1.

3.2.1 Standard Volterra expansion

The kernels $\epsilon_0^{(1)}(s_1)$ and $\epsilon_0^{(2)}(s_1, s_2)$ have been derived as indicated in the Appendix and are shown in Figs. 1b (solid line) and 4. Figure 5 shows a small section of the spike train of Fig. 3a with a single spike. Two intervals, one before (lower left) and a second during and immediately after the spike (lower right) are shown on an enlarged scale. Before the spike occurs, the numerical solution of the Hodgkin-Huxley equations (solid) is well approximated by the first-order Volterra expansion $u(t) = \int ds\, \epsilon_0^{(1)}(s)\, I(t-s)$ (long dashed) and even better by the second-order approximation (dotted). During a spike, however, even an approximation to third order fails completely; cf. Fig. 6.

The discrepancy during a spike may be surprising at a first sight but is not completely unexpected. During action potential generation, the neuronal dynamics is mainly driven by internal processes of channel opening and closing, much more than by external input. Mathematically, the reason is that the series expansion is valid only as long as $I(t)$ is not too large; see the Appendix.

3.2.2 Expansion including action potentials

In order to account for the remaining differences, we have to add explicitly the shape of the spike and the afterpotential by way of the kernel $\eta_1(s)$. The function $\eta_1(s)$ has been determined by the procedure explained in Section 2 and is shown

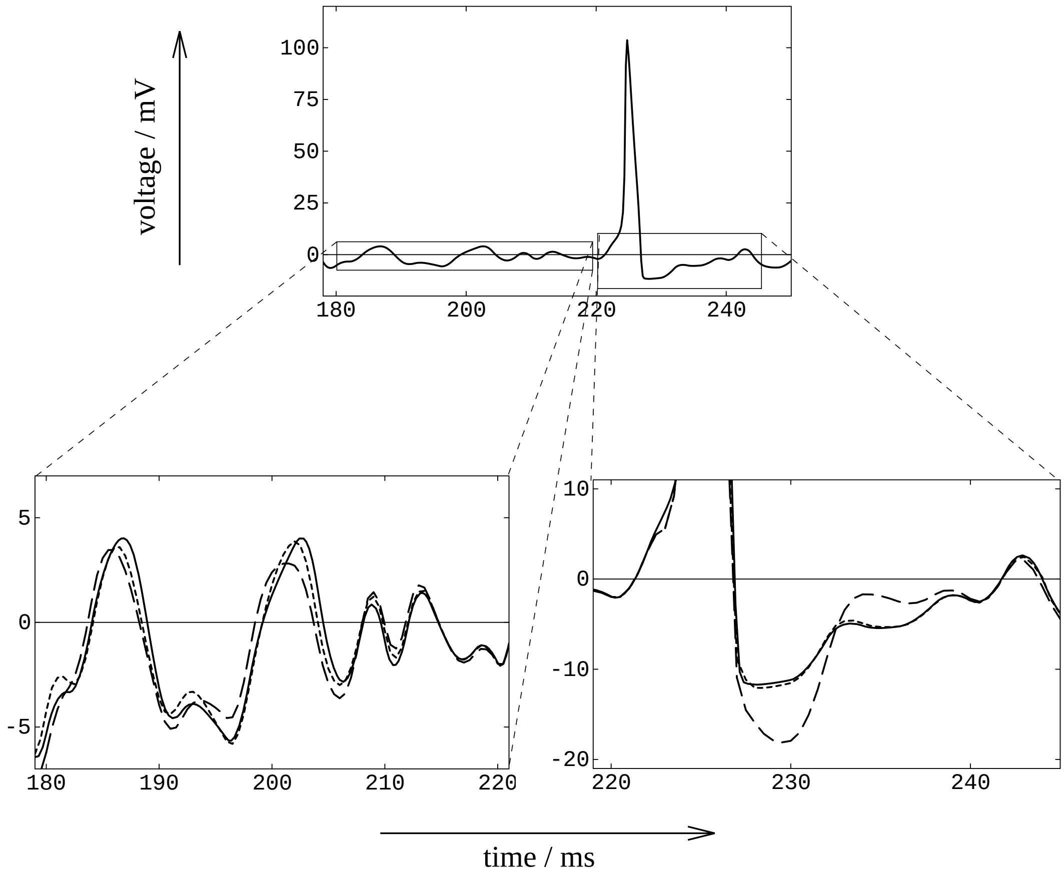

Figure 5: Systematic approximation of the Hodgkin-Huxley model by the spike-response model (3). The upper graph of Fig. 5 shows a small section of the Hodgkin-Huxley spike train of Fig. 3a. The lower left diagram shows the solution of the Hodgkin-Huxley equations (solid) and the first (dashed) and second (dotted) order approximation with the kernels $\epsilon_0^{(1)}$ and $\epsilon_0^{(2)}$ before the spike occurs on an enlarged scale. The lower right diagram illustrates the behavior of the membrane immediately after an action potential. The solution of the Hodgkin-Huxley equations (solid line) is approximated by $u(t) = \eta_1(t - t^f) + \int ds\, \epsilon_0^{(1)}(s)\, I(t - s)$, a dashed line. Using the improved kernel $\epsilon_1^{(1)}$ instead of $\epsilon_0^{(1)}$ results in a nearly perfect fit (dotted line).

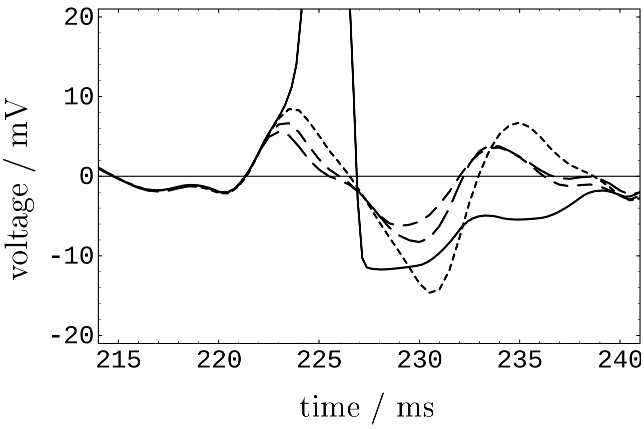

Figure 6: Approximation of the Hodgkin-Huxley model by a standard Volterra expansion (2) during a spike. Here we demonstrate the importance of the kernel η_1 as it appears in (3). First- (long dashed) and second-order approximation (dashed) using the kernels $\epsilon_0^{(1)}$ and $\epsilon_0^{(2)}$ produce a significant peak in the membrane potential where the Hodgkin-Huxley equations generate an action potential (solid line), but even the third-order approximation (dotted) fails to reproduce the spike with a peak of nearly 100 mV (far out of scale). The remaining difference is taken care of by the kernel η_1.

in Fig. 1a. If we add $\eta_1(t - t^f)$ but continue to work with the standard kernels $\epsilon_0^{(1)}(s)$, $\epsilon_0^{(2)}(s, s')$, ... we find large errors in an interval up to roughly 20 ms after a spike. This is exemplified in the lower right of Fig. 5 where the long-dashed line shows the approximation $u(t) = \eta_1(t - t^f) + \int ds\, \epsilon_0^{(1)}(s)\, I(t - s)$. From a biological point of view, this is easy to understand. The kernel $\epsilon_0^{(1)}(s)$ describes a postsynaptic potential in response to a standard input. Due to refractoriness, the responsiveness of the membrane is lower after a spike and for this reason the postsynaptic potential looks different, if an input pulse arrives shortly after an output spike. We then have to work with the improved kernels $\epsilon_1^{(1)}(\sigma; s)$, $\epsilon_1^{(2)}(\sigma; s, s')$, ... introduced in Eq. (3). The dotted line in the lower-right graph of Fig. 5 gives the approximation $u(t) := \eta_1(t - t^f) + \int ds\, \epsilon_1^{(1)}(t - t^f; s)\, I(t - s)$ and we see that the fit is nearly perfect.

3.2.3 Threshold criterion

The trigger time t^f of an action potential is given by a simple threshold crossing process. Although the expansion in terms of the ϵ kernels will never give the perfect form of the spike, the truncated series expansion does exhibit rather significant peaks at positions where the Hodgkin-Huxley model produces spikes (Fig. 6). We have therefore decided to apply a simple *voltage* threshold criterion instead of using some other derived quantity such as the derivative $\dot{v}$ or an 'effective input current' (Koch et al. 1995). Whenever the membrane potential in terms of the expansion (3) reaches the threshold ϑ from below, we define a firing time t^f and add a contribution $\eta(t-t^f)$. The threshold parameter ϑ is considered as a fit parameter and has to be optimized as described below. This finishes the definition of the spike response model.

4 Simulation results

We have compared the full Hodgkin-Huxley model and the spike response model (3) in a simulation of spike activity over 100 000 ms, i.e., 100 s. In so doing, we have accepted a spike of the spike response model to be *coincident* with the corresponding spike of the Hodgkin-Huxley model if it arrives within a temporal precision of ± 2 ms.

4.1 Coincidence measure

As a measure of the rate of coincidence of spikes generated by the Hodgkin-Huxley equations and another model such as (3), we define an index Γ that is the number of coincidences minus the number of coincidences 'by chance' relative to the total number of spikes produced by the Hodgkin-Huxley and the other model. More precisely, Γ is the fraction

$$\Gamma = \frac{N_{\text{coinc}} - \langle N_{\text{coinc}} \rangle}{\frac{1}{2}(N_{\text{HH}} + N_{\text{SRM}})} \mathcal{N}^{-1}. \tag{13}$$

Here N_{coinc} is the number of coincident spikes of Hodgkin-Huxley and the other model as counted in a single simulation run, N_{HH} the number of action potentials generated by the Hodgkin-Huxley equations, and N_{SRM} the number of spikes produced by model, say, (3). The normalization factor $\mathcal{N}$ restricts Γ to unity in the case of a perfect coincidence of the other model's spike train with the Hodgkin-Huxley one ($N_{\text{coinc}} = N_{\text{SRM}} = N_{\text{HH}}$). Finally, $\langle N_{\text{coinc}} \rangle$ is the average number of coincidences obtained, if the spikes of our model were not generated systematically but randomly by a homogeneous Poisson process. Hence $\Gamma \approx 0$, if (3) would produce spikes 'randomly'. The definition (13) is a modification of an idea of Joeken and Schwegler (1995).

In order to calculate $\langle N_{\text{coinc}} \rangle$, we perform a gedanken experiment. we are-given the numbers N_{HH} and N_{SRM} and divide the total simulation time into K bins of 4 ms length each. Due to refractoriness, each bin contains at most one Hodgkin-Huxley spike; we denote the number of these bins by N_{HH}. So $(K - N_{\text{HH}})$ bins are empty. We now distribute N_{SRM} *randomly* generated spikes among the K bins, each bin receiving at most one spike. A coincidence occurs each time a bin contains a Hodgkin-Huxley spike *and* a random spike. The probability to encounter $N_{\rm coinc}$ coincidences is thus hypergeometrically distributed, i.e., $p(N_{\rm coinc}) = \binom{N_{\rm HH}}{N_{\rm coinc}} \binom{K-N_{\rm HH}}{N_{\rm SRM}-N_{\rm coinc}} / \binom{K}{N_\vartheta}$, with mean $\langle N_{\rm coinc} \rangle = N_{\rm SRM}\, N_{\rm HH} \,/\, K$. To see why, we use a simple analogy. Imagine we have an urn with $N_{\rm HH}$ 'black' balls and $(K - N_{\rm HH})$ 'white' balls, and perform a random sampling of $N_{\rm SRM}$ balls *without* replacement. The number of black balls drawn from the urn corresponds to the number of coincidences in the original problem. This setup is governed by the hypergeometric distribution (Prohorov and Rozanov 1969, Feller 1970). In passing we note that dropping the 'refractory' side condition leads to a binomial distribution and, hence, tothe very same result for $\langle N_{\rm coinc} \rangle$.

Using the correct normalization, i.e., $\mathcal{N} = 1 - N_{\rm HH} \,/\, K$, we thus obtain a suitable measure: Γ has expectation zero for a purely random spike train, yields unity in case of a perfect coincidence of the spike response model's spike train with the Hodgkin-Huxley one, and is bounded by -1 from below. A negative Γ hints at a negative correlation. Furthermore, Γ is linear in the number of coincidences and monotonically decreasing with the number of erroneous spikes. That is, Γ decreases with increasing $N_{\rm SRM}$ while $N_{\rm coinc}$ is kept fixed or with decreasing $N_{\rm coinc}$ while N_ϑ is kept fixed.

While simulating the spike response model we have found that due to the long-lasting afterpotential a single misplaced spike causes subsequent spikes to occur with high probability at false times too. Since this is not a numerical artifact but a well-known and even experimentally observed biological effect (Mainen and Sejnowski 1995), we have adopted the following procedure in order to eliminate this type of 'error' from the statistics. Every time the spike response model fails to reproduce a spike of the Hodgkin-Huxley spike train we note an error and add the kernel η at the position where the original Hodgkin-Huxley spike occurred. Analogously, we count an error and omit the afterpotential if the spike response model produces a spike where no spike should occur. In case of a coincidence between the Hodgkin-Huxley spike and a spike of the spike response model we take no action, i.e., we place the η kernel at the position suggested by the threshold criterion. Without correction, Γ would decrease by at most a few percent and the standard deviation would increase by a factor two.

4.2 Low firing rate

The results of the simulations for low mean firing rates have been summarized in Table 2. Due to the large interspike intervals, effects from spikes in the past are rather weak. Hence we can ignore the dependence of the ϵ kernels upon the former firing times and work with $\epsilon_0^{(1)}(s)$ instead of $\epsilon_1^{(1)}(\sigma; s)$. We do, however, take into account the kernel $\eta_1(s)$. Higher-order kernels $\epsilon_0^{(2)}$, $\epsilon_0^{(3)}$ give a significant improvement over an approximation with $\epsilon_0^{(1)}$ only. This reflects the importance of the nonlinear interaction of input pulses. In a third-order approximation the spike-response model reproduces 85 percent of the Hodgkin-Huxley spikes correctly, cf. Table 2.

4.3 High firing rate

At higher firing rates the influence of the most recent *output* spike is more important than the nonlinear interaction between *input* pulses. We, therefore, use the kernel $\epsilon_1^{(1)}$ but neglect higher-order terms with $\epsilon_1^{(2)}$, $\epsilon_1^{(3)}$, ... in Eq. (3). Figure 7 gives the results of the simulations with different mean firing rates. As for Table 2, the threshold ϑ and the time δ between the formal threshold crossing time t^f and the maximum of the action potential have been optimized in a separate run over 10 s. For this optimization run we have used an input current with $\sigma = 3\,\mu\text{A/cm}^2$, corresponding to a mean firing rate of about 33 Hz; the maximum mean firing rate is here in the range of 70 Hz.

For firing rates above 30 Hz, the single-variable model reproduces about 90 percent of the Hodgkin-Huxley spikes correctly. This is quite remarkable since we have only used the *first*-order approximation

$$u(t) = \eta(t - t^f) + \int \mathrm{d}s\, \epsilon_1^{(1)}(t - t^f; s)\, I(t - s) \tag{14}$$

and neglected all higher-order terms. If we would neglect the influence of last spike we would end up with a coincidence rate of only 73 percent, even in a second-order approximation using kernels $\epsilon_0^{(1)}$ and $\epsilon_0^{(2)}$.

Closer examination of the simulation results for various mean firing rates reveals a systematic deviation of the mean firing rate of the spike-response model from the mean firing rate of the Hodgkin-Huxley equations. More precisely, the spike response model generates additional spikes where no spike should occur, and misses less spikes if the standard deviation of the input current is increased – after all, quite natural (Mainen and Sejnowski 1995).

We have performed the same test with two versions of traditional integrate-and-fire models, namely a simple integrate-and-fire model with reset potential u_0 and time constant τ, and an integrate-and-fire model with time-dependent threshold derived from the η-kernel found by the methods described in Sec. 2.4, viz., $\vartheta(\sigma) = -\eta_1(\sigma)$ for $\sigma > 5\,\text{ms}$ and $\vartheta(\sigma) = \infty$ for $\sigma < 5\,\text{ms}$. The results are summarized in Fig. 8. We have optimized the parameters τ, ϑ_0 and u_0 with a fluctuating input current as explained above and found optimal performance for a time constant of $\tau = 1\,\text{ms}$. This surprisingly short time constant should be compared to the time constants of the $\epsilon_1^{(1)}$ kernel. Indeed, if the time since the

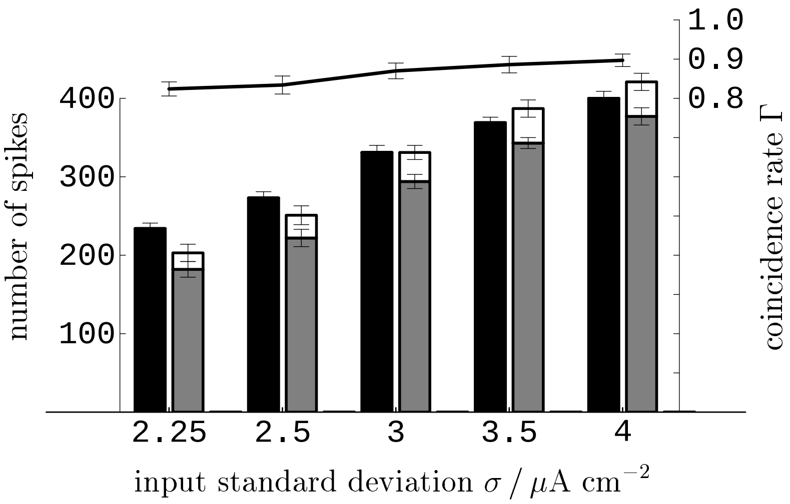

Figure 7: Simulation results for different mean firing rates using the *first*-order improved kernel $\epsilon_1^{(1)}$ *only.* The black bars indicate the number of spikes (left axis) produced by the Hodgkin-Huxley model, the neighboring bars correspond to the number of spikes of the spike response model. The gray shading reflects the coincident spikes. All numbers are averages of 10 runs over 10 s with different realizations of the input current. The mean firing rate varies between 23 and 40 Hz. The error bars are the corresponding standard deviations. The line in the upper part of the diagram indicates the coincidence rate Γ (right axis) as defined by Eq. (13). The parameters $\vartheta = 4.7\,\text{mV}$ and $\delta = 2.15\,\text{ms}$ have been optimized in a separate run with an input current with standard deviation $\sigma = 3\,\mu\text{A cm}^{-2}$.

order	ϑ / mV	δ / ms	$N_{\rm SRM}$	$N_{\rm coinc}$	$N_{\rm wrong}$	$N_{\rm missed}$	Γ
first	4.00	2.85	91 ± 8	71 ± 7	20 ± 5	16 ± 3	0.788 ± 0.030
second	4.70	2.75	87 ± 11	74 ± 8	13 ± 3	13 ± 2	0.845 ± 0.016
third	5.80	2.50	88 ± 10	76 ± 8	13 ± 3	11 ± 3	0.858 ± 0.019

Table 2: Simulation results of the spike response model using the Volterra kernels $\epsilon_0^{(1)}$, ..., $\epsilon_0^{(3)}$. The table gives the number of spikes produced by the spike response model ($N_{\rm SRM}$), the number of coincidences ($N_{\rm coinc}$), the number of spikes produced by the spike response model where no spike should occur ($N_{\rm wrong}$) and the number of missing spikes ($N_{\rm missed}$). The numbers give the average and standard deviation after 10 runs with different realizations of the input current and a duration of 10 s per run. The numbers should be compared with the number of spikes in the Hodgkin-Huxley model, $N_{\rm HH} = 87 \pm 8$. The coincidence rate Γ has been defined by Eq. (13). For random gambling we would obtain $\Gamma \approx 0$. The parameters ϑ (threshold) and δ (time from threshold crossing to maximum of the action potential) have been determined by optimizing the results in a separate run over 10 s.

last spike is shorter than about 10 ms, cf. Fig. 1b, the $\epsilon_1^{(1)}$ kernel approaches zero within a few milliseconds. The optimized reset value was $u_0 = -3\,\text{mV}$ and the threshold $\vartheta_0 = 3.05\,\text{mV}$ resp. $\vartheta_0 = 2.35\,\text{mV}$ for the model with respectively without time-dependent threshold.

4.4 Response to current step functions

Constant input currents have been a paradigm to neuron models ever since Hodgkin and Huxley (1952), even though a constant current is very far from reality and one may wonder wether it offers a sensible criterion for the behavior of neurons producing *spikes* and, thus, responding to *fluctuating* input currents. Nevertheless we want to study the response of our model to current steps and compare it with that of the original Hodgkin-Huxley model.

As a consequence of the oscillatory behavior of the first-order kernel $\epsilon_0^{(1)}$ (see Fig. 1b), our model exhibits a phenomenon known as *inhibitory rebound.* Suppose we have a constant inhibitory, i.e. negative, input current for time $t < 0$ which is turned off suddenly at $t = 0$. We can easily calculate the membrane potential from Eq. (1) if we assume that there are no spikes in the past. The resulting voltage trace exhibits a significant oscillation (Fig. 9). If the current step is large enough, the positive overshooting triggers a single spike after the release of

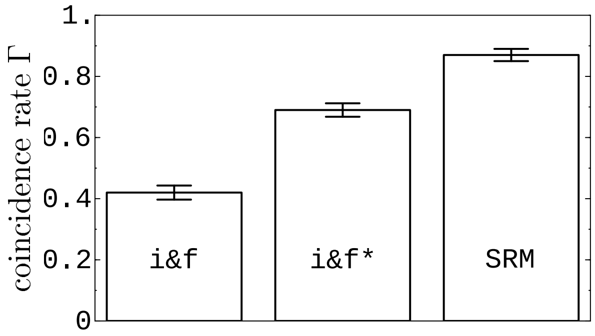

Figure 8: Comparison of various threshold models. The diagram shows the coincidence rate Γ defined in Sec. 4.1 for a simple integrate-and-fire model with time constant $\tau = 1\,\mathrm{ms}$ and reset potential $u_0 = -3\,\mathrm{mV}$ (i&f), an integrate-and-fire model with time-dependent threshold (i&f*), and the spike-response model (SRM). The error bars indicate the standard deviation of 10 simulations over 10 s each with a fluctuating input current with $\sigma = 3\,\mu\mathrm{A}\ \mathrm{cm}^{-2}$.

the inhibition. Since (1) is linear in the input, the amplitude of the oscillatory response of the membrane potential in Fig. 9 is proportional to the *height* of the current step but independent of the absolute current values before or after the step. This is in contrast to the Hodgkin-Huxley-equations, where amplitude and frequency of the oscillations depend both on step height and absolute current values (Mauro et al. 1970).

The limitations of a voltage threshold for spike prediction can be investigated by systematically studying the response of the model to current steps; cf. Fig. 10. For $t < 0$ we apply a constant current with amplitude I_1. At at $t = 0$ we switch to a stronger input $I_2 > I_1$. Depending on the values of the final input current I_2 and the step height $\Delta I = I_2 - I_1$ we observe three different modes of behavior in the original Hodgkin-Huxley model, as is well-known (Cronin 1987). For small steps and low final input currents, the membrane potential exhibits a transient oscillation but *no* spikes (inactive phase I). Larger steps can induce a *single* spike immediately after the step (single spike phase S). Increasing the final input current further leads to repetitive firing (R). Note that repetitive firing is possible for $I > 6\,\mu\mathrm{A}\ \mathrm{cm}^{-2}$, but firing must be triggered by a sufficiently large current step ΔI. Only for currents larger than $9.47\,\mu\mathrm{A}/\mathrm{cm}^2$ there is autonomous firing independently of the current step. We conclude from the above step response behavior that there are two different threshold paradigms, namely a single-spike threshold (dashed line in Fig. 10) and a threshold for repetitive firing (solid line).

We want to compare the above results with the behavior of our threshold model. The same set of step response simulations has been performed with the spike response model. Comparing the threshold lines in the $(I_2, \Delta I)$-diagram

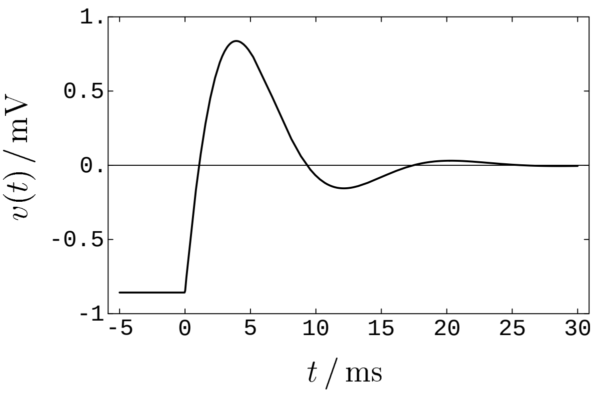

Figure 9: Response of the spike response model to a current step. An inhibitory input current which is suddenly turned off produces a characteristic oscillation of the membrane potential. The overshooting membrane potential can trigger an action potential immediately after the inhibition is turned off. The amplitude of the oscillation is proportional to the height of the current step. Here, the current is switched from -1 μA cm^{-2} to 0 at time $t = 0$.

for the Hodgkin-Huxley model and the spike response model, we can state a qualitative correspondence. The spike response model exhibits the very same three modes of response as the Hodgkin-Huxley equations. Let us have a closer look at the two thresholds, the single spike threshold and the repetitive firing threshold. The slope of the single-spike threshold (dashed line in Fig. 10) is far from being perfect, if we compare the lower and the upper part of the figure. The slope is determined by the mean $\int \mathrm{d}s\, \epsilon_0^{(1)}(s)$ of the linear response kernel $\epsilon_0^{(1)}$ and is therefore fixed as long as we stick to the membrane voltage as the relevant variable used in applying the threshold criterion.

We now turn to the threshold of repetitive firing. The position of the vertical branch of the repetitive-firing threshold (solid line in Fig. 10) is shifted to lower current values as compared to the Hodgkin-Huxley model. Consequently, the gain function of the spike response model is shifted to lower current values too (Fig. 11). The repetitive-firing threshold is directly related to the (free) threshold parameter ϑ and can be moved to larger current values by increasing ϑ. Using $\vartheta = 9\,\mathrm{mV}$ instead of $\vartheta = 4.7\,\mathrm{mV}$ results in a reasonable fit of the Hodgkin-Huxley gain function (Fig. 11). However, a shift of ϑ would also shift the single-spike threshold of Fig. 10 to larger current values and the triggering of single spikes at low currents would be made practically impossible. The value for the threshold parameter $\vartheta = 4.7\,\mathrm{mV}$ found by optimization with a fluctuating input as described in Sec. 4.3 is therefore a compromise.

It follows from Fig. 10 that there is not a strict voltage threshold for spiking in the Hodgkin-Huxley model. Nevertheless, our model qualitatively exhibits all relevant phases and, with the fluctuating input scenario, there is even a fine

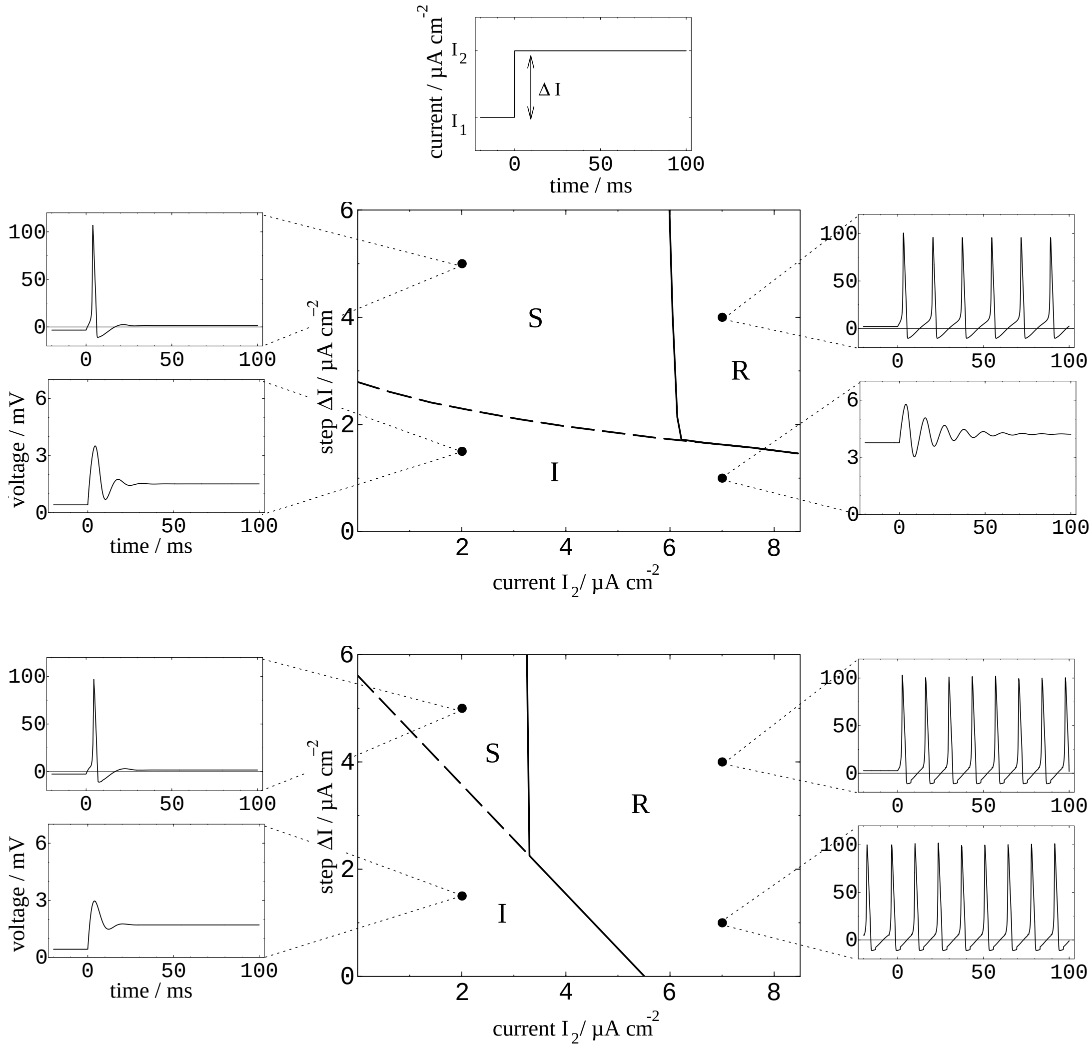

Figure 10: Comparison of the response to current steps of the Hodgkin-Huxley equations (upper graph) and of the spike response model (lower graph). At time $t = 0$ the input current is switched from I_1 to I_2 and the behavior of the models is studied in dependence upon the final current I_2 and the step height $\Delta I = I_2 - I_1$. The figures in the center indicate in the manner of a phase diagram three different regimes: (I) the neuron remains inactive; (S) a single spike is triggered; (R) repetitive firing is induced. We have chosen four representative pairs of values of I_2 and ΔI (marked by dots in the phase diagram) and plotted the corresponding time course of the membrane potential on the left and the right of the main diagram so that the responses of Hodgkin-Huxley model and spike response model can be compared. The parameters for the spike response model are the same as those detailed in the caption to Table 3.

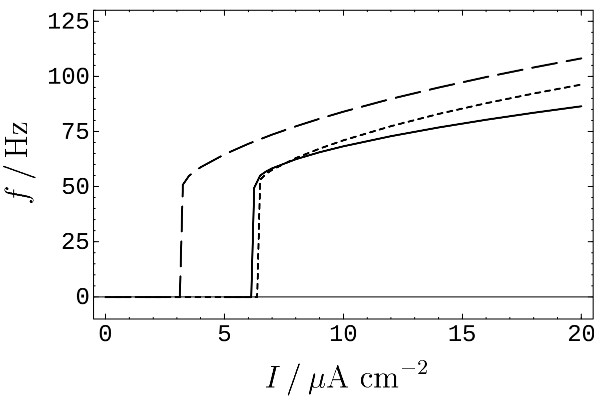

Figure 11: Comparison of the gain function (output firing rate for constant input current I as a function of I) of the spike-response and the Hodgkin-Huxley model. The threshold parameter $\vartheta = 4.7\,\mathrm{mV}$ found by the optimization procedure described in Sec. 4.3 gives a gain function of the spike response model (dashed line) that is shifted towards lower current values as compared to the gain function of the Hodgkin-Huxley model (solid line). Increasing the threshold parameter to $\vartheta = 9\,\mathrm{mV}$ results in a reasonable fit (dotted line).

quantitative agreement.

5 Discussion

In contrast to the complicated dynamics of the Hodgkin-Huxley equations, the spike response model (3) has a straightforward and intuitively appealing interpretation. Furthermore, the transparent structure of the spike response model has a great number of advantages. The dynamical behavior of a single neuron can be discussed in simple but 'biological' terms of threshold, postsynaptic potential, refractoriness, and afterpotential. Let us discuss the issue by way of a few examples.

As a first example, we discuss the refractory period. Refractoriness of the Hodgkin-Huxley model leads to two distinct effects. On the one hand, we have shunting effects, i.e., a reduced responsiveness of the membrane to input spikes during and immediately after the spike. This is related to absolute refractoriness and is expressed in our model by the first argument of $\epsilon_1^{(1)}$. In addition, the kernel η_1 induces an afterpotential which corresponds to a relative refractory period. In the Hodgkin-Huxley model, the afterpotential corresponds with hyperpolarization and lasts for about 15 ms followed by a rather small depolarization. We mention that a different form of the afterpotential with a significant depolarizing phase would lead to intrinsic bursting (Gerstner and van Hemmen 1992). So the neuronal behavior is easily taken care of by the spike response model.

a

b

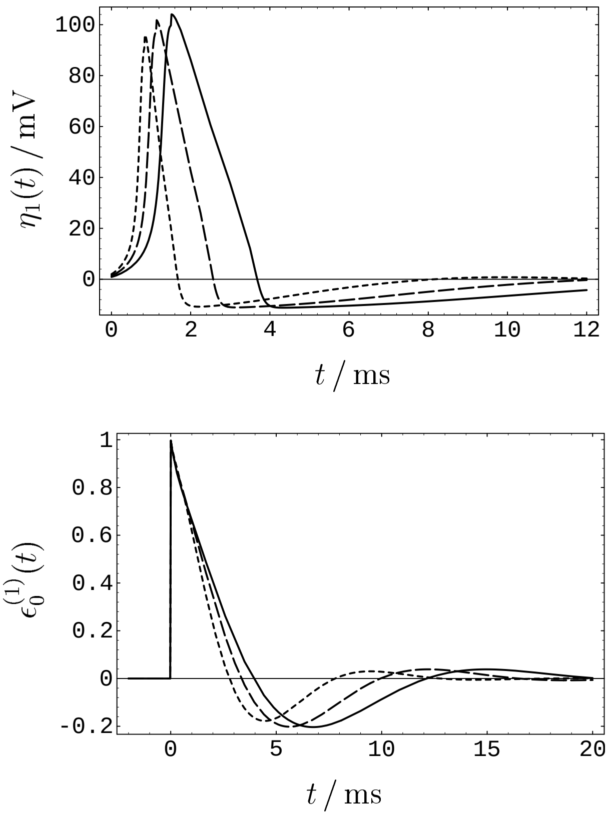

Figure 12: Temperature dependence of the kernels corresponding to the Hodgkin-Huxley equations. Both η_1 kernel (*a*) and $\epsilon_0^{(1)}$ kernel (*b*) show apart from a stretching in time no significant change in form if temperature is decreased from 15.0 (dotted line) and 10.0 (dashed line) to 6.3 (solid line) degrees Celsius.

As a second example, let us focus on the temperature dependence of the various kernels. Temperature can be included in the Hodgkin-Huxley equations by multiplying the right-hand side of (12) by a temperature-dependent factor ζ (Cronin 1987),

$$\zeta = \exp\left[\ln(3.0)\,(T - 6.3)\,/\,10.0\right] \tag{15}$$

with the temperature T in degrees Celsius. Equation (11) remains unmodified. In Fig. 12 we have plotted the resulting $\epsilon_0^{(1)}$ and η_1 kernels for different temperatures. Although the temperature correction affects only the equations for m, h and n, the overall effect can be approximated by a time rescaling, since the form of both kernels is not modified but stretched in time with decreasing temperature.

Apart from the transparent structure, the single-variable model is open to a mathematical analysis which would be unconceivable for the full Hodgkin-Huxley equations. Most importantly, the collective behavior of a large network of neurons can now be predicted, if the form of the kernels η and $\epsilon^{(1)}$ is known (Gerstner and van Hemmen 1993, Gerstner 1995, Gerstner et al. 1996). In particular, the existence and stability of collective oscillations can be studied by a simple graphical construction using the kernels η and $\epsilon^{(1)}$. It can be shown that a collective oscillation is stable, if the sum of the postsynaptic potentials is *increasing* at the moment of firing. Otherwise it is unstable (Gerstner et al. 1996). Furthermore, it can be shown that in a fully connected and homogeneous network of spike-response neurons with a potential described by (1), the state of asynchronous firing is almost always unstable (Gerstner 1995). Also in simulations of a network of Hodgkin-Huxley neurons a spontaneous break up of the asynchronous firing state and a small oscillatory component in the mean firing activity has been observed (Wang 1995).

Summarizing: We have used the Hodgkin-Huxley equations as a well-studied reference model of spike dynamics and shown that it can indeed be reduced to a threshold model. Our methods are, however, more general and can also be applied to more elaborate models that involve many ion currents and a complicated spatial structure. Furthermore, an *analytic* evaluation of some of the kernels – see the Appendix for mathematical details – is possible. We have also presented a numerical algorithm to determine the response kernels that, in contrast to the Wiener method, can be determined fast and easily. In fact, the spike response method which we have used in our analysis can be seen as a systematic approach to a reduction of a complex system to a threshold model.

Acknowledgments: This work has been supported by the Deutsche Forschungsgemeinschaft (DFG) under grant numbers He 1729/2-2 and 8-1.

A Appendix

In this Appendix we treat Volterra's theory (Volterra 1959) in the context of inhomogeneous differential equations, indicate under what conditions and how the kernels of the Volterra series can be computed analytically, and isolate the mathematical essentials of our own approach.

A.1 Volterra Series

We start by studying the ordinary differential equation

$$\dot{x} - f(x) = j, \tag{16}$$

where j is a given function of time and $\dot{x}$ denotes differentiation of $x(t)$ with respect to t. We require that for $j \equiv 0$, $x = 0$ should be an attractive fixed point with a sufficiently large basin of attraction so that the system returns to equilibrium if the perturbation $j(t)$ is turned off. Furthermore, we require f and j to be continuous and bounded and f to fulfill a Lipschitz condition. Finally, $j \in \mathcal{L}^2(\mathbb{R})$ should have compact support so that $x \in \mathcal{L}^2(\mathbb{R})$.

Under these premises there exists a unique solution x, with $x(-\infty) = 0$ for each input $j \in \mathcal{A} \subset \mathcal{L}^2(\mathbb{R})$. Hence, the time course of the solution x is a function[1] of the time course of the perturbation j, formally,

$$\begin{aligned} &F : \mathcal{A} \subset \mathcal{L}^2(\mathbb{R}) \to \mathcal{L}^2(\mathbb{R}), \\ &\qquad j \mapsto F[j] = x \quad \text{with} \quad \dot{x}(t) - f(x(t)) = j(t), \ \forall\, t \in \mathbb{R}. \end{aligned} \tag{17}$$

Let us suppose that the function F is analytic in a neighborhood of the constant solution $x \equiv 0$. For a precise definition of the notion of 'analyticity' and conditions under which it holds, we refer to Thomas (1996). Then there is a Taylor series (Dieudonné 1968, Dunford and Schwartz 1958, Kolmogorov and Fomin 1975, Hille and Phillips 1957) for F,

$$F[j] = 0 + F'[0][j] + \frac{1}{2!} F''[0][j,j] + \ldots \tag{18}$$

This series is convergent with respect to the $\|.\|_2$-norm, i.e., $F[j](t) = x(t)$ for almost all $t \in \mathbb{R}$. Each derivative $F^{(n)}[0]$ in (18) is a continuous n-linear mapping from $\left(\mathcal{L}^2(\mathbb{R})\right)^n$ to $\mathcal{L}^2(\mathbb{R})$. Hence, $F^{(n)}[0][.](t) : \left(\mathcal{L}^2(\mathbb{R})\right)^n \to \mathbb{R}$ is a continuous n-linear functional for almost all (fixed) $t \in \mathbb{R}$. We know that every such functional has a Volterra-like integral representation (Volterra 1959, Palm and Poggio 1977, Palm 1978),

$$F^{(n)}[0][j](t) = \int \mathrm{d}t_1 \ \ldots \int \mathrm{d}t_n \ \epsilon_t^{(n)}(t_1, \ldots, t_n)\, j(t-t_1) \ldots j(t-t_n). \tag{19}$$

In the most general case the kernels $\epsilon_t^{(n)}$ are distributions. We will see, however, that the kernels describing (17) are (almost everywhere) continuous functions from $\mathcal{L}^2(\mathbb{R}^n)$.

Combination of (18) and (19) yields the Volterra-series of F,

$$\begin{aligned} x(t) \ = \ & \int \mathrm{d}t_1 \ \epsilon^{(1)}(t_1)\ j(t-t_1) \ + \\ & + \frac{1}{2!} \int \mathrm{d}t_1 \int \mathrm{d}t_2 \ \epsilon^{(2)}(t_1, t_2)\ j(t-t_1)\ j(t-t_2) \ + \ \ldots \ + \\ & + \frac{1}{n!} \int \mathrm{d}t_1 \ldots \int \mathrm{d}t_n \ \epsilon^{(n)}(t_1, \ldots, t_n)\ j(t-t_1) \ldots j(t-t_n) \ + \\ & + \ \ldots \end{aligned} \tag{20}$$

[1]Note the chosen bracket convention: (..) denotes the dependence upon a real or complex scalar while [..] denotes the dependence upon a function.

Because we expand around the constant solution $x \equiv 0$, the ϵ kernels do not depend on the time t but on the difference $(t - t^\star)$, $t^\star$ being the time when we have stated the initial condition. In this subsection, we calculate the solution for the initial condition $x(t^\star = -\infty) = 0$ and the ϵ kernels do not depend on t at all. We have therefore dropped the index t from $\epsilon_t^{(n)}$ as it occurs in (19). As is discussed in Section A.3 below, dropping the index is possible only if no spike occurs in the past.

We can easily generalize this formalism to systems of differential equations,

$$\dot{x_k} - f_k(x_1, \ldots, x_N) = \delta_{k,1}\, j(t), \quad k = 1, \ldots, N, \tag{21}$$

and obtain

$$x_k(t) = \int dt_1\, \epsilon_k^{(1)}(t_1)\, j(t-t_1) + \frac{1}{2!}\int \mathrm{d}t_1 \int \mathrm{d}t_2\, \epsilon_k^{(2)}(t_1, t_2)\, j(t-t_1)\, j(t-t_2) + \ldots \tag{22}$$

As opposed to the lower index t in (19), and the lower index p in (4), the subscript k in (22) denotes the k-th vector component of the system throughout the rest of this appendix.

A.2 Calculation of the kernels

We want to prove that the kernels $\epsilon_0^{(1)}$, $\epsilon_0^{(2)}$, ... can be calculated explicitly for fairly arbitrary systems of differential equations. In particular, it is possible to obtain analytic expressions for the kernels in terms of the eigenvalues of the linearization of the N-dimensional system of differential equations we start with.

Suppose f in (16) is analytic in a neighborhood of $x = 0$ so that we can expand f in a Taylor series around $x = 0$. In doing so, we use the Einstein summation convention. We substitute the Taylor series into (21),

$$\dot{x_k} - \left(\frac{\partial f_k}{\partial x_l} x_l + \frac{1}{2!} \frac{\partial^2 f_k}{\partial x_l \partial x_m} x_l x_m + \ldots \right) = \delta_{k,1} j(t), \quad k = 1, \ldots, N, \tag{23}$$

realize that the derivatives are evaluated at $x = 0$, and switch to Fourier transforms,

$$i\, \omega\, x_k(\omega) - \left(\frac{\partial f_k}{\partial x_l} x_l(\omega) + \frac{1}{2!} \frac{\partial^2 f_k}{\partial x_l \partial x_m} \int d\omega_1\, x_l(\omega - \omega_1)\, x_m(\omega_1) + \ldots \right) = \\ = \delta_{k,1}\, j(\omega). \tag{24}$$

The Fourier transform of the Volterra series (22) is

$$x_k(\omega) = \epsilon_k^{(1)}(\omega)\, j(\omega) + \frac{1}{2!} \int d\omega_1\, \epsilon_k^{(2)}(\omega - \omega_1, \omega_1)\, j(\omega - \omega_1)\, j(\omega_1) + \ldots \tag{25}$$

We substitute this into (24) and obtain a polynomial (in a convolution algebra) in terms of $j(\omega)$,

$$
\begin{aligned}
0 \;=\; & \left[c_k + c_{kl}(\omega)\epsilon_l^{(1)}(\omega)\right]\; j(\omega) \;+ \\
& + \int d\omega_1 \;\left[\frac{1}{2}c_{kl}(\omega)\;\epsilon_l^{(2)}(\omega-\omega_1,\omega_1) + c_{klm}\;\epsilon_l^{(1)}(\omega-\omega_1)\;\epsilon_m^{(1)}(\omega_1)\right] \times \\
& \qquad\qquad\qquad j(\omega-\omega_1)\; j(\omega_1) \;+ \\
& + \int d\omega_1 \int d\omega_2 \left[\frac{1}{6}c_{kl}(\omega)\;\epsilon_l^{(3)}(\omega-\omega_1-\omega_2,\omega_1,\omega_2) + /.../\right] \times \\
& \qquad\qquad\qquad j(\omega-\omega_1-\omega_2)\; j(\omega_1)\; j(\omega_2) \;+\; \ldots
\end{aligned}
\tag{26}
$$

Here we have defined the abbreviations $c_k = \delta_{k,1}$,

$$
c_{kl}(\omega) = \frac{\partial f_k}{\partial x_l} - i\;\omega\delta_{k,l}\;, \tag{27}
$$

and

$$
c_{klm} = \frac{1}{2!}\frac{\partial^2 f_k}{\partial x_l \partial x_m}\,, \quad c_{klmn} = \frac{1}{3!}\frac{\partial^3 f_k}{\partial x_l \partial x_m \partial x_n}\,, \quad \ldots \tag{28}
$$

Equation (26) holds for every function j. The coefficients of $j(\omega)$ therefore have to vanish identically and we are left with a set of *linear* equations for the kernels, which can be solved consecutively,

$$
\begin{aligned}
c_{kl}(\omega)\;\epsilon_l^{(1)}(\omega) \;&=\; -c_k\;, \\
c_{kl}(\omega_1+\omega_2)\;\epsilon_l^{(2)}(\omega_1,\omega_2) \;&=\; -2\;c_{klm}\;\epsilon_l^{(1)}(\omega_1)\;\epsilon_m^{(1)}(\omega_2)\;, \\
c_{kl}(\omega_1+\omega_2+\omega_3)\;\epsilon_l^{(3)}(\omega_1,\omega_2,\omega_3) \;&=\; -6\;c_{klmn}\;\epsilon_l^{(1)}(\omega_1)\;\epsilon_m^{(1)}(\omega_2)\;\epsilon_n^{(1)}(\omega_3) - \\
&\qquad -\;3\;c_{klm}\left[\epsilon_l^{(1)}(\omega_1)\epsilon_m^{(2)}(\omega_2,\omega_3) + \right. \\
&\qquad\qquad \left. +\;\epsilon_m^{(1)}(\omega_2)\epsilon_l^{(2)}(\omega_1,\omega_3)\right]\;, \\
&\;\;\vdots
\end{aligned}
\tag{29}
$$

Note that we have to invert *only one* matrix, viz. $c_{kl}(\omega)$, in order to solve (29) for *all* kernels. The inverse of $c_{kl}(\omega)$ is

$$
c_{mn}^{-1}(\omega) = \frac{1}{\det c_{kl}(\omega)}\;C_{nm}(\omega), \tag{30}
$$

where $C_{nm}(\omega)$ is the adjunct matrix of $c_{kl}(\omega)$ defined in (27).

Solving (29) we obtain for $\epsilon_k^{(n)}(\omega_1,\ldots,\omega_n)$ an expression with a denominator that is a product of the characteristic polynomial $p(\omega) := \det c_{kl}(\omega)$, evaluated at different frequencies ω. For instance, solving (29) for $\epsilon_k^{(2)}(\omega_1,\omega_2)$ yields a denominator $p(\omega_1)\,p(\omega_2)\,p(\omega_1+\omega_2)$, and the denominator in $\epsilon_k^{(3)}(\omega_1,\omega_2,\omega_3)$ is $p(\omega_1)\,p(\omega_2)\,p(\omega_3)\,p(\omega_1+\omega_3)\,p(\omega_2+\omega_3)\,p(\omega_1+\omega_2+\omega_3)$, etc. If we know the roots of $p(\omega)$, i.e., the eigenvalues of the system of differential equations, we can factorize the denominator and easily determine the residues of $\epsilon_k^{(n)}(\omega_1,\ldots,\omega_n)$ and, thus, derive an analytic expression for the inverse Fourier transform of $\epsilon_k^{(n)}(\omega_1,\ldots,\omega_n)$, viz.,

$$\epsilon_k^{(n)}(t_1,\ldots,t_n) = \theta(t_1,\ldots,t_n)\,\sum_l a_{kl}\,\exp\left[\nu_{kl1}\,t_1+\ldots+\nu_{kln}\,t_n\right]. \tag{31}$$

The coefficients $\nu_{klm}\in\mathbb{C}$ are sums and differences of the N eigenvalues λ_k of the N-dimensional system of differential equations,

$$\nu_{klm} = \varsigma_{klm1}\,\lambda_1+\ldots+\varsigma_{klmN}\,\lambda_N, \quad \varsigma\in\{-1,0,1\}. \tag{32}$$

The computational difficulties are reduced to the calculation of the N roots of a polynomial of degree N where N is the system dimension; cf. (21).

A.3 Limitations

In most cases, the function F is not an entire function, i.e., the series expansion around the constant solution $x\equiv 0$ does not converge for all perturbations j (Thomas 1996). For the Hodgkin-Huxley equations we have found numerically that the truncated series expansion gives a fine approximation to the true solution *only* as long as the input current keeps well below the spiking threshold. This is not too surprising, since the solution of Hodgkin-Huxley equations exhibits an apparent discontinuity at spiking threshold. Consider a family of input functions given by

$$j_\tau : t\mapsto j_0\,\theta(t-\tau)\,\theta(t+\tau). \tag{33}$$

These are square pulses with height j_0 and duration 2τ. There is a threshold $j_\vartheta(\tau)$ and a small constant δ with $\delta\,/\,j_\vartheta(\tau)\ll 1$ so that for $j_0 < j_\vartheta(\tau)-\delta$ no spike occurs, whereas for $j_0 > j_\vartheta(\tau)+\delta$ at least one spike is triggered within a given compact interval, cf. Fig. 2. Thus, the 2-norm of the derivative, $\|F'[j_\tau]\|_2\approx \|F[j_\tau+\delta]-F[j_\tau-\delta]\|_2\,/\,2\delta$, takes large values as j_0 approaches the value $j_\vartheta(\tau)$ and we do not expect the series expansion to converge beyond that point.

In the main part of this paper we have introduced the response function η in order to address this problem. The key advantage of η_1 and the 'improved' kernels $\epsilon_1^{(1)}$, $\epsilon_1^{(2)}$, ... is that we no longer expand around the constant solution $x\equiv 0$ but around a solution of the Hodgkin-Huxley equations that contains a single spike at $t=t^f$. In the context of Eq. (20), we have argued that the ϵ kernels do not depend on the absolute time. Since, however, the new zero-order approximation $u(t) = \eta_1(t - t^f)$ contains a spike, homogeneity of time is destroyed and the improved ϵ kernels depend on $(t - t^f)$ where t^f is the latest firing time. Unfortunately, there is no analytic solution for the Hodgkin-Huxley equations with spikes. We therefore have to, and did, resort to numerical methods in order to determine the kernel $\epsilon_1^{(n)}$ in the neighborhood of a spike.

In order to construct approximations of solutions with more than one spike, we have to concatenate these single-spike approximations. We can then exploit the fact that the truncated series expansion exhibits rather prominent peaks in the membrane potential at positions where the Hodgkin-Huxley equations would produce a spike. The task is to decide from the truncated series expansion which of the peaks in the approximated membrane potential belong to a spike and which do not. In the main body of the paper we have investigated how well this can be done by using a threshold criterion.

References

Abbott L. F., Kepler T. B., 1990, Model neurons: from Hodgkin-Huxley to Hopfield. In Garrido L., editor, *Statistical Mechanics of Neural Networks.* Springer, Berlin.

Abbott L. F., Vreeswijk C. van, 1993, Asynchronous states in a network of pulse-coupled oscillators. *Phys. Rev. E*, 48:1483–1490.

Av-Ron E., Parnas H., Segel L. A., 1991, A minimal biophysical model for an excitable and oscillatory neuron. *Biol. Cybern.*, 65:487–500.

Cronin J., 1987, *Mathematical aspects of Hodgkin-Huxley theory.* Cambridge University Press, Cambridge.

Dieudonné J., 1968, *Foundations of modern analysis*, chapter 8.14. Academic Press, New York.

Dunford N., Schwartz J. T., 1958, *Linear operators, Part I: General Theory*, chapter III.14. Wiley, New York.

Ekeberg O., Wallen P., Lansner A., Traven H., Brodin L., Grillner S., 1991, A computer based model for realistic simulations of neural networks. *Biol. Cybern.*, 65:81–90.

Feller W., 1970, *An introduction to probability theory and its applications*, volume I, chapter II.6. Wiley, New York, 3rd edition.

FitzHugh R., 1961, Impulses and physiological states in models of nerve membrane. *Biophys. J.*, 1:445–466.

Gerstner W., 1991, Associative memory in a network of 'biological' neurons. In Lippmann R. P., Moody J. E., Touretzky D. S., editors, *Advances in Neural Information Processing Systems 3*, pp. 84–90, San Mateo CA. Morgan Kaufmann Publishers.

Gerstner W., 1995, Time structure of the activity in neural network models. *Phys. Rev. E*, 51:738–758.

Gerstner W., Hemmen J. L. van, 1992, Associative memory in a network of ‘spiking’ neurons. *Network*, 3:139–164.

Gerstner W., Hemmen J. L. van, 1993, Coherence and incoherence in a globally coupled ensemble of pulse emitting units. *Phys. Rev. Lett.*, 71(3):312–315.

Gerstner W., Hemmen J. L. van, Cowan J. D., 1996, What matters in neuronal locking? *Neural Comput.*, 8:1689–1712.

Hille E., Phillips R. S., 1957, *Functional Analysis and Semi-Groups*, chapter III. American Mathematical Society, Providence, RI.

Hodgkin A. L., Huxley A. F., 1952, A quantitative description of ion currents and its applications to conduction and excitation in nerve membranes. *J. Physiol. (London)*, 117:500–544.

Hopfield J. J., Herz A. V. M., 1995, Rapid local synchronization of action potentials: towards computation with coupled integrate-and-fire networks. *Proc. Natl. Acad. Sci. USA*, 92:6655.

Joeken S., Schwegler H., 1995, Predicting spike train responses of neuron models. In Verleysen M., editor, *Proc. 3rd European Symposium on Artificial Neural Networks*, pp. 93–98, Brussels. D facto.

Kepler Thomas B., Abbott L. F., Marder Eve, 1992, Reduction of conductance-based neuron models. *Biol. Cybern.*, 66:381–387.

Kernell D., Sjöholm H., 1973, Repetitive impulse firing: comparison between neuron models based on voltage clamp equations' and spinal motoneurons. *Acta Physiol. Scand.*, 87:40–56.

Koch C., Bernander Ö., Douglas R. J., 1995, Do neurons have a voltage or a current threshold for action potential initiation? *J. Comput. Neurosci.*, 2:63–82.

Kolmogorov A. N., Fomin S. V., 1975, *Reelle Funktionen und Funktionalanalysis*, chapter 10. VEB Deutscher Verlag der Wissenschaften, Berlin.

Korenberg M. J., 1989, A robust orthogonal algorithm for system identification and time-series analysis. *Biol. Cybern.*, 60:267–276.

Lapicque L., 1907, Recherches quantitatives sur l'excitation electrique des nerfs traitée comme une polarisation. *J. Physiol. Pathol. Gen.*, 9:620–635.

Mainen Z. F., Sejnowski T. J., 1995, Reliability of spike timing in neocortical neurons. *Science*, 268:1503–1506.

Mauro A., Conti F., Dodge F., Schor R., 1970, Subthreshold behavior and phenomenological impedance of the giant squid axon. *J. Gen. Physiol.*, 55:497–523.

Palm G., 1978, On representation and approximation of nonlinear systems. *Biol. Cybernetics*, 31:119–124.

Palm G., Poggio T., 1977, The Volterra representation and the Wiener expansion: Validity and pitfalls. *SIAM J. Appl. Math.*, 33(2):195–216.

Palm G., Poggio T., 1978, Stochastic identification methods for nonlinear systems: An extension of the Wiener theory. *SIAM J. Appl. Math.*, 34(3):524–534.

Prohorov Yu. V., Rozanov Yu. A., 1969, *Probability*, chapter I-5.3. Springer, Berlin.

Rinzel J., 1985, Excitation dynamics: insights from simplified membrane models. *Federation Proc.*, 44:2944–2946.

Thomas E. G. F., 1996, Q-Analytic solution operators for non-linear differential equations. *Preprint, Dept. of Mathematics, University of Groningen.*

Traub R. D., Wong R. K. S., Miles R., Michelson H., 1991, A model of a CA3 hippocampal pyramidal neuron incorporating voltage-clamp data on intrinsic conductances. *J. Neurophysiol.*, 66:635–650.

Tsodyks M., Mitkov I., Sompolinsky H., 1993, Patterns of synchrony in inhomogeneous networks of oscillators with pulse interaction. *Phys. Rev. Lett.*, 71:1281–1283.

Usher M., Schuster H. G., Niebur E., 1993, Dynamics of populations of integrate-and-fire neurons, partial synchronization and memory. *Neural Computation*, 5:570–586.

Volterra V., 1959, *Theory of functionals and of integral and integro-differential equations.* Dover, New York.

Wang, 1995. private communication.

Wiener N., 1958, *Nonlinear problems in random theory.* M.I.T. Press, Cambridge, MA.

Wilson M. A., Bhalla U. S., Uhley J. D., Bower J. M., 1989, Genesis: A system for simulating neural networks. In Touretzky D., editor, *Advances in Neural Information Processing Systems*, pp. 485–492, San Mateo, CA. Morgan Kaufmann Publishers.

Yamada W. M., Koch C., Adams P. R., 1989, Multiple channels and calcium dynamics. In Koch C., Segev I., editors, *Methods in neuronal modeling: From synapses to networks*, Cambridge, MA. MIT Press.